

Robust Anomaly Detection Under Normality Distribution Shift in Dynamic Graphs

Xiaoyang Xu
xu.xiaoyang.42r@st.kyoto-u.ac.jp
Kyoto University
Kyoto, Japan

Xiaofeng Lin
lxf@ml.ist.i.kyoto-u.ac.jp
Kyoto University
Kyoto, Japan

Koh Takeuchi
takeuchi@i.kyoto-u.ac.jp
Kyoto University
Kyoto, Japan

Kyohei Atarashi
atarashi@i.kyoto-u.ac.jp
Kyoto University
Kyoto, Japan

Hisashi Kashima
kashima@i.kyoto-u.ac.jp
Kyoto University
Kyoto, Japan

Abstract

Anomaly detection in dynamic graphs is a critical task with broad real-world applications, including social networks, e-commerce, and cybersecurity. Most existing methods assume that normal patterns remain stable over time; however, this assumption often fails in practice due to the phenomenon we refer to as normality distribution shift (NDS), where normal behaviors evolve over time. Ignoring NDS can lead models to misclassify shifted normal instances as anomalies, degrading detection performance. To tackle this issue, we propose WhENDS, a novel unsupervised anomaly detection method that aligns normal edge embeddings across time by estimating distributional statistics and applying whitening transformations. Extensive experiments on four widely-used dynamic graph datasets show that WhENDS consistently outperforms nine strong baselines, achieving state-of-the-art results and underscoring the importance of addressing NDS in dynamic graph anomaly detection. The codes are available at <https://anonymous.4open.science/r/WhENDS>.

CCS Concepts

• Security and privacy → Intrusion/anomaly detection and malware mitigation.

Keywords

Anomaly Detection, Dynamic Graphs, Out-of-Distribution

ACM Reference Format:

Xiaoyang Xu, Xiaofeng Lin, Koh Takeuchi, Kyohei Atarashi, and Hisashi Kashima. 2025. Robust Anomaly Detection Under Normality Distribution Shift in Dynamic Graphs. In . ACM, New York, NY, USA, 11 pages. <https://doi.org/10.1145/nnnnnnn.nnnnnnn>

Permission to make digital or hard copies of all or part of this work for personal or classroom use is granted without fee provided that copies are not made or distributed for profit or commercial advantage and that copies bear this notice and the full citation on the first page. Copyrights for components of this work owned by others than the author(s) must be honored. Abstracting with credit is permitted. To copy otherwise, or republish, to post on servers or to redistribute to lists, requires prior specific permission and/or a fee. Request permissions from permissions@acm.org.
Conference'17, Washington, DC, USA

© 2025 Copyright held by the owner/author(s). Publication rights licensed to ACM.
ACM ISBN 978-x-xxxx-xxxx-x/YYYY/MM
<https://doi.org/10.1145/nnnnnnn.nnnnnnn>

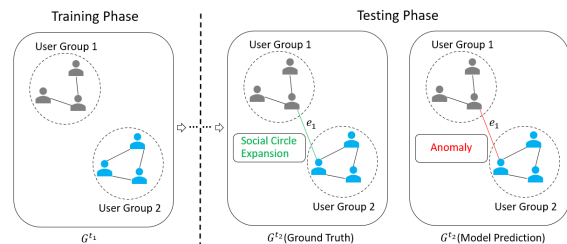


Figure 1: A toy example illustrating how normality distribution shift (NDS) affects model performance. During training, two groups of users have no inter-group connections. In the test phase, a new edge e_1 (in green) emerges due to natural behavioral evolution, such as the expansion of social circles. Although e_1 should be considered normal, it deviates from the normal pattern learned during training and is thus mistakenly classified as an anomaly (in red).

1 Introduction

Anomaly detection, which aims to identify patterns in data that deviate from expected norms [6], is a fundamental task with critical applications across various domains. For instance, in social networks, interactions among benign users represent normal behavior, while activities such as fraud, cyberbullying, phishing, and rumor propagation are considered anomalies. Accurately detecting such anomalies is vital for ensuring system security and maintaining platform integrity.

In many real-world scenarios, data can be naturally modeled as dynamic graphs—graph-structured data whose topology and features evolve over time. Typical examples include social networks [4, 31], financial systems [38, 44], and traffic networks [20]. As a result, anomaly detection in dynamic graphs has emerged as an important and actively studied problem. Due to the scarcity of labeled anomalies, most existing dynamic graph anomaly detection methods [13, 22, 34] adopt an unsupervised approach: they learn the distribution of normal patterns from training data and detect anomalies as deviations from this distribution during testing.

Although existing approaches have shown promising performance, they typically assume that normal patterns remain stable

over time. In reality, however, normal behavior may evolve—a phenomenon we refer to as *normality distribution shift (NDS)*. For example, in social networks, benign user behavior may vary due to seasonal trends, emerging events, or natural expansion of social circles. As illustrated in Figure 1, the presence of NDS means that even normal samples may deviate from the patterns learned during training, potentially leading models to misclassify them as anomalies.

To tackle this challenge, we propose a novel anomaly detection method for dynamic graphs, called **Whitening of Edge distribution for Normality Distribution Shift (WhENDS)**. WhENDS estimates the distributional statistics of normal edge embeddings at each timestamp and uses them to perform whitening. This alignment transforms normal edge embeddings across time into a common standard Gaussian distribution, thereby mitigating the impact of NDS.

We summarize the main contributions of this work as follows:

- We identify and formalize the challenge of normality distribution shift (NDS) in dynamic graph anomaly detection, and empirically demonstrate its significant impact on model performance.
- We propose **WhENDS**, a novel unsupervised anomaly detection method that mitigates NDS by estimating and whitening the distribution of normal edge embeddings over time.
- Extensive experiments on benchmark datasets show that WhENDS outperforms state-of-the-art methods and remains robust under various levels of NDS.

2 Related Work

2.1 Anomaly Detection in Dynamic Graphs

As an important task in dynamic graphs, anomaly detection has attracted significant research attention. Early methods primarily relied on traditional machine learning techniques. For example, GOutlier [1] identifies anomalies by analyzing structural connectivity patterns, and CM-Sketch [27] leverages approximated anomaly metrics derived from empirical statistics to detect abnormal edges.

In recent years, the strong performance of deep learning has made it the dominant paradigm for dynamic graph anomaly detection. NetWalk [34] adopts a reconstruction-based strategy by training an autoencoder on random walk sequences to generate node and edge embeddings, and evaluates anomaly scores through clustering these embeddings. AddGraph [43] leverages GCN [17] to encode graph information and employs an attention mechanism along with GRU [8] to capture both short-term and long-term temporal dependencies. StrGNN [5] encodes h-hop enclosing subgraphs using GCN and aggregates temporal information with GRU. TADDY [22] utilizes edge-based substructure sampling and a Transformer [29] to obtain spatial-temporal encodings of dynamic graphs. RustGraph [13] integrates GNNs with GRUs to aggregate temporal information and introduces VGAE [16] and graph contrastive learning to better encode dynamic graphs.

Despite their success, existing dynamic graph anomaly detection methods generally assume that the distribution of normal patterns remains stationary over time. They do not explicitly consider the possibility of NDS, where the normal pattern can change over time.

As a result, these methods may misclassify shifted normal samples as anomalies, leading to performance degradation under NDS.

2.2 Graph Out-Of-Distribution (OOD) Generalization

To address distribution shift in graph data, numerous Graph OOD generalization methods have been proposed. These methods can be broadly categorized into three groups [37]: data-augmentation-based methods [11, 28, 33, 42], generalizable model-based methods [21, 23], and learning strategy-based methods [15, 39]. However, most of these studies focus on static graphs and fail to capture the crucial temporal information inherent in dynamic graphs, making them unsuitable for direct application to dynamic settings.

In an effort to handle distribution shift in dynamic graphs, several recent works have explored OOD generalization methods specifically for dynamic graphs [35, 40, 41]. Nevertheless, these approaches typically rely on large amounts of labeled data for training, which limits their applicability to anomaly detection in dynamic graphs, where labeled anomalies are scarce or unavailable.

Despite these efforts in generalizing the OOD of graphs, the aforementioned limitations prevent existing methods from being directly applied to anomaly detection in dynamic graphs to address the problem of NDS, which motivates the design of our proposed method.

3 Problem Formulation

Let $\mathbb{G} = \{\mathcal{G}^1, \mathcal{G}^2, \dots, \mathcal{G}^T\}$ be a dynamic graph with maximum timestamp T , where each snapshot \mathcal{G}^t at timestamp t is defined as $\mathcal{G}^t = \{\mathcal{V}^t, \mathcal{E}^t\}$, with \mathcal{V}^t denoting the node set and \mathcal{E}^t the edge set. For attributed graphs, we use $\{A^t, X^t\}$, where $A^t \in \mathbb{R}^{N^t \times N^t}$ is the adjacency matrix such that $A^t_{ij} = 1$ if an edge e^t_{ij} exists between nodes v^t_i and v^t_j , and 0 otherwise; $X^t \in \mathbb{R}^{N^t \times d}$ denotes the node feature matrix, where $N^t = |\mathcal{V}^t|$ and d is the feature dimension. Over time, both \mathcal{V}^t , \mathcal{E}^t , and node attributes may evolve.

To distinguish between normal and anomalous edges in each snapshot \mathcal{G}^t , we denote the sets of normal and anomalous edges as $\mathcal{E}^t_{\text{norm}}$ and $\mathcal{E}^t_{\text{ano}}$, respectively. We define *normality distribution shift (NDS)* in a dynamic graph as a temporal change in the distribution of normal edges. Let $\mathcal{D}^t_{\text{norm}}$ represent the distribution of normal edges $e^t_{ij} \in \mathcal{E}^t_{\text{norm}}$ at timestamp t . Then, NDS occurs if $\mathcal{D}^t_{\text{norm}} \neq \mathcal{D}^{t_2}_{\text{norm}}$ for any $t_1 \neq t_2$.

Following prior work [5, 13, 22, 43], we adopt an unsupervised setting for anomaly detection in dynamic graphs. Specifically, the data in the training phase are assumed to be entirely normal and unlabeled; we use the first K snapshots $\mathbb{G}_{\text{tr}} = \{\mathcal{G}^1, \dots, \mathcal{G}^K\}$ as the training set. During testing, we inject synthetic anomalous edges into the remaining snapshots $\mathbb{G}_{\text{te}} = \{\mathcal{G}^{K+1}, \dots, \mathcal{G}^T\}$ to evaluate model performance.

Our goal is to learn an anomaly detection function $f(\cdot)$ using only the training data. Given an edge e^t_{ij} , the model outputs an anomaly score $f(e^t_{ij}) \in [0, 1]$, representing the likelihood that the edge is anomalous. The model should assign low scores to normal edges and high scores to anomalous ones, and maintain robustness even under NDS.

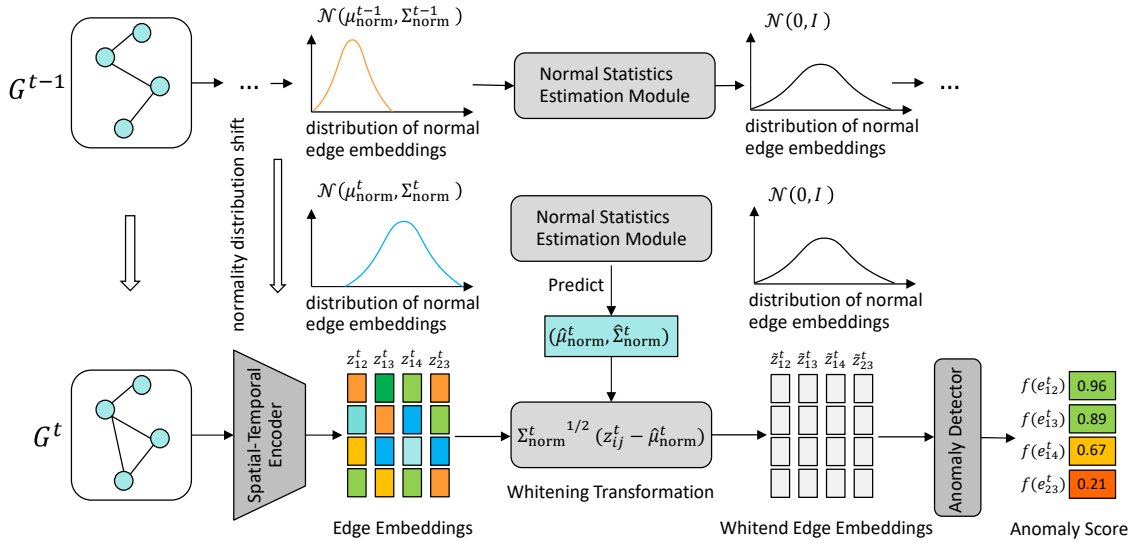


Figure 2: Overview of WhENDS. The framework consists of three main modules: a Spatial-Temporal Encoder, a Normal Statistics Estimation Module (NSEM), and an Anomaly Detector. At each timestamp, the input graph snapshot is processed by the Spatial-Temporal Encoder to obtain edge embeddings, which are then whitened using predicted statistics from the NSEM. The whitened embeddings are passed to the Anomaly Detector to compute anomaly scores for each edge. By aligning normal edge embeddings at all timestamps to a standard Gaussian distribution, the NSEM mitigates the effects of normality distribution shift.

4 Proposed Method

In this section, we present the components of our proposed method, **WhENDS**, as illustrated in Figure 2. WhENDS is composed of three key modules: (1) the **Spatial-Temporal Encoder**, which captures spatial-temporal patterns in dynamic graphs and generates edge embeddings; (2) the **Normal Statistic Estimation Module (NSEM)**, which estimates the distributional statistics of normal edge embeddings and performs whitening to align them with a standard Gaussian distribution at each timestamp; and (3) the **Anomaly Detector**, which assigns an anomaly score to each edge based on the whitened embeddings.

We begin by detailing the Normal Statistic Estimation Module, the core component of WhENDS responsible for mitigating the effects of NDS.

4.1 Normal Statistics Estimation Module

To model the distribution of normal edges and address the challenge of NDS, we make the following approximation: at any timestamp t , the embeddings of normal edges can be approximately modeled by a multivariate Gaussian distribution $\mathcal{N}(\mu_{\text{norm}}^t, \Sigma_{\text{norm}}^t)$. While this approximation may not perfectly capture all real-world edge distributions, it provides a principled and efficient basis for mitigating NDS in dynamic graphs. Under this approximation, if the parameters $(\mu_{\text{norm}}^t, \Sigma_{\text{norm}}^t)$ can be obtained, a whitening transformation can be applied to align the normal edge embeddings at each timestamp to a standard Gaussian distribution $\mathcal{N}(0, I)$, thus mitigating the impact of NDS.

Since the true statistics of normal edge embeddings are not directly accessible in the testing phase, we design the Normal Statistics Estimation Module (NSEM) to estimate the statistics of normal edge embeddings $(\mu_{\text{norm}}^t, \Sigma_{\text{norm}}^t)$ at each timestamp t , as illustrated in Figure 3. NSEM leverages data augmentation to learn the deviation between the overall edge distribution and the normal edge distribution in the presence of anomalies. Additionally, a GRU is employed to model the evolving pattern of the distribution of normal edges. The estimated statistics are then used to perform whitening on the edge embeddings.

Data Augmentation for Normal Statistics Estimation. In the training phase, there is no anomalous edge present. Therefore, for each snapshot G^t in the training set, the distribution of all edges in G^t is equivalent to that of the normal edges at timestamp t , i.e.,

$$\mathcal{D}_{\text{all}}^t = \mathcal{D}_{\text{norm}}^t, \quad \text{if } t \leq K. \quad (1)$$

In contrast, in the testing phase, due to the presence of anomalous edges, the distribution over all edges in G^t becomes

$$\mathcal{D}_{\text{all}}^t = \mathcal{D}_{\text{norm}}^t \cup \mathcal{D}_{\text{ano}}^t, \quad \text{if } t > K. \quad (2)$$

The presence of anomalies causes the overall edge embedding statistics (denoted as $(\mu_{\text{all}}^t, \Sigma_{\text{all}}^t)$) to deviate from the normal edge distribution. Denote $\Delta\mu^t, \Delta\Sigma^t$ as this deviation:

$$\Delta\mu^t = \mu_{\text{all}}^t - \mu_{\text{norm}}^t, \quad (3)$$

$$\Delta\Sigma^t = \Sigma_{\text{all}}^t - \Sigma_{\text{norm}}^t. \quad (4)$$

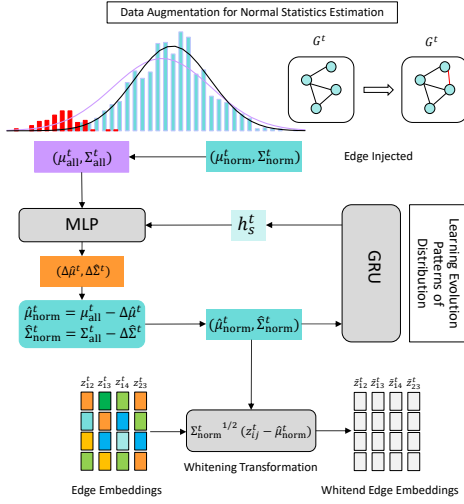


Figure 3: Normal Statistics Estimation Module. The NSEM consists of an MLP and a GRU. Given the overall statistics as input, the MLP estimates the deviation from normal statistics and recovers the clean normal statistics, which are then used to whiten the edge embeddings at the current timestamp. The predicted normal statistics are also passed to the GRU to update its hidden state, allowing the model to capture temporal evolution and improve predictions at subsequent timestamps.

To solve this, a natural idea is to estimate and subtract this deviation $\Delta\mu^t, \Delta\Sigma^t$ in order to recover the normal statistics $(\mu_{\text{norm}}^t, \Sigma_{\text{norm}}^t)$ from the corrupted observations. To achieve this, we simulate the presence of anomalies via data augmentation on the training set. Specifically, for each training snapshot, we randomly inject α (sampled from 1% to 10%) of synthetic edges, which are treated as anomalous. We then use a multi-layer perceptron (MLP) to predict $(\Delta\mu^t, \Delta\Sigma^t)$ on the augmented snapshot:

$$\Delta\hat{\mu}^t, \Delta\hat{\Sigma}^t = \text{MLP}(\mu_{\text{all}}^t \oplus \text{Flatten}(\text{Chol}(\Sigma_{\text{all}}^t))) \oplus h_s^{t-1}, \quad (5)$$

where \oplus denotes the concatenation operator, $\text{Chol}(\cdot)$ denotes the Cholesky decomposition that extracts the lower triangular matrix, and $\text{Flatten}(\cdot)$ denotes the operation that flattens a matrix into a one-dimensional vector. With the predicted deviations $\Delta\hat{\mu}^t$ and $\Delta\hat{\Sigma}^t$, we recover the estimated statistics of normal edge embeddings as:

$$\hat{\mu}_{\text{norm}}^t = \mu_{\text{all}}^t - \Delta\hat{\mu}^t, \quad (6)$$

$$\hat{\Sigma}_{\text{norm}}^t = (\Sigma_{\text{all}}^t - \Delta\hat{\Sigma}^t)(\Sigma_{\text{all}}^t - \Delta\hat{\Sigma}^t)^\top. \quad (7)$$

In the above equations, $(\Sigma_{\text{all}}^t - \Delta\hat{\Sigma}^t)(\Sigma_{\text{all}}^t - \Delta\hat{\Sigma}^t)^\top$ is designed to ensure that $\hat{\Sigma}_{\text{norm}}^t$ is positive definite, which guarantees the validity of the subsequent whitening transformation.

Learning Evolution Patterns of Distribution. In our design, NSEM is trained using augmented data in which random edges are inserted into the training snapshots to simulate anomalies. However, in practice, the actual anomalies in the test set may differ

significantly from the synthetic ones introduced through data augmentation. When such a mismatch occurs, the accuracy of NSEM's predictions can be compromised. To mitigate this limitation, as many prior studies have shown that evolving data distributions often follow certain temporal patterns [26, 32, 36], we aim to learn such evolution pattern of the normal edge distribution as auxiliary information to guide the estimation process. By doing so, NSEM is no longer solely dependent on the data augmentation strategy, but can leverage historical trends in normality to improve robustness and generalization. To this end, we employ a Gated Recurrent Unit (GRU) [8] to model the evolution pattern of normal edge distributions and update the hidden states h_s^t in Equation (5):

$$\mathbf{x}_s^t = \mu_{\text{norm}}^t \oplus \text{Flatten}(\text{Chol}(\Sigma_{\text{norm}}^t)), \quad (8)$$

$$\mathbf{z}_s^t = \sigma(W_{xz}\mathbf{x}_s^t + W_{hz}\mathbf{h}_s^t), \quad (9)$$

$$\mathbf{r}_s^t = \sigma(W_{xr}\mathbf{x}_s^t + W_{hr}\mathbf{h}_s^t), \quad (10)$$

$$\mathbf{h}'_s{}^t = \tanh(W_{xh}\mathbf{x}_s^t + W_{hh}\mathbf{h}_s^t), \quad (11)$$

$$\mathbf{h}_s^t = (1 - \mathbf{z}_s^t) \circ \mathbf{h}_s^{t-1} + \mathbf{z}_s^t \circ \mathbf{h}'_s{}^t, \quad (12)$$

where \circ denotes the Hadamard product and $\sigma(\cdot)$ represents the sigmoid function.

Whitening Transformation. In the testing phase, we apply the predicted normal statistics to perform a whitening transformation [2] on each edge embedding, aligning it to a standard Gaussian distribution. The whitening transformation is computed as

$$\tilde{z}_{ij}^t = (\hat{\Sigma}_{\text{norm}}^t)^{-\frac{1}{2}}(z_{ij}^t - \hat{\mu}_{\text{norm}}^t), \quad (13)$$

where z_{ij}^t denotes the edge embedding of edge e_{ij}^t and \tilde{z}_{ij}^t denotes the whitened edge embedding. $(\hat{\Sigma}_{\text{norm}}^t)^{-\frac{1}{2}}$ denotes the inverse square root of the covariance matrix $\hat{\Sigma}_{\text{norm}}^t$.

Finally, we train NSEM by minimizing the difference between the predicted and ground-truth statistics of normal edges. The Statistics Loss is defined as

$$\mathcal{L}_{\text{statistics}} = \|\hat{\mu}_{\text{norm}}^t - \mu_{\text{norm}}^t\|_2^2 + \|\hat{\Sigma}_{\text{norm}}^t - \Sigma_{\text{norm}}^t\|_2^2. \quad (14)$$

4.2 Spatial-Temporal Encoder

While representation learning on dynamic graphs is an important and challenging problem in its own right, it is not the main focus of this work. Therefore, we adopt a simplified adaptation of GC-LSTM [7] to capture the temporal and spatial information critical to anomaly detection, which we find sufficient for learning expressive edge embeddings in our anomaly detection framework. At each timestamp t , the input and output of the Spatial-Temporal Encoder are computed as

$$\mathbf{x}^t = \text{GNN}_x(\mathbf{X}^t), \quad (15)$$

$$\mathbf{f}^t = \sigma(\text{GNN}_{xf}(\mathbf{x}^t, \mathbf{A}^t) + \text{GNN}_{hf}(\mathbf{h}^{t-1}, \mathbf{A}^{t-1})), \quad (16)$$

$$\mathbf{i}^t = \sigma(\text{GNN}_{xi}(\mathbf{x}^t, \mathbf{A}^t) + \text{GNN}_{hi}(\mathbf{h}^{t-1}, \mathbf{A}^{t-1})), \quad (17)$$

$$\mathbf{o}^t = \sigma(\text{GNN}_{xo}(\mathbf{x}^t, \mathbf{A}^t) + \text{GNN}_{ho}(\mathbf{h}^{t-1}, \mathbf{A}^{t-1})), \quad (18)$$

$$\mathbf{z}^t = \tanh(\text{GNN}_{xz}(\mathbf{x}^t, \mathbf{A}^t) + \text{GNN}_{hz}(\mathbf{h}^{t-1}, \mathbf{A}^{t-1})), \quad (19)$$

$$\mathbf{c}^t = (\mathbf{f}^t \mathbf{c}^{t-1}) + (\mathbf{i}^t \mathbf{z}^t), \quad \mathbf{n}^t = (\mathbf{f}^t \mathbf{n}^{t-1}) + \mathbf{i}^t, \quad (20)$$

$$\mathbf{h}^t = \mathbf{o}^t (\mathbf{c}^t / \mathbf{n}^t), \quad \mathbf{Z}_{\text{node}}^t = \mathbf{h}^t, \quad (21)$$

where $\text{GNN}(\cdot)$ denotes a graph neural network, X^t and A^t are the feature matrix and adjacency matrix of the snapshot \mathcal{G}^t , respectively, and $Z_{\text{node}}^t \in \mathbb{R}^{N^t \times d}$ represents the node embeddings at timestamp t . In addition, \mathbf{n}^t is a normalizer state [3] used to stabilize the hidden state \mathbf{h}^t , preventing large numerical fluctuations that could hinder NSEM from accurately learning and predicting the distributional statistics. Let \mathbf{z}_i^t denote the i -th row of Z_{node}^t , representing the representation of node i at timestamp t . For an edge $e_{ij}^t \in \mathcal{E}^t$, its edge embedding \mathbf{z}_{ij}^t is computed as $\mathbf{z}_{ij}^t = \mathbf{z}_i^t + \mathbf{z}_j^t$.

The Spatial-Temporal Encoder is trained via a graph reconstruction task, where we aim to reconstruct both the feature matrix X^t and the adjacency matrix A^t from the learned node embeddings Z_{node}^t . The reconstructions are given by:

$$\hat{X}^t = \text{MLP}(Z_{\text{node}}^t), \quad \hat{A}^t = \sigma(Z_{\text{node}}^t Z_{\text{node}}^{t \top}). \quad (22)$$

Then the reconstruction loss is defined as

$$\mathcal{L}_{\text{recon}} = \|\hat{X}^t - X^t\|_F^2 + \|\hat{A}^t - A^t\|_F^2, \quad (23)$$

where $\|\cdot\|_F$ denotes the Frobenius norm.

4.3 Anomaly Detector

After obtaining the node embeddings from the Spatial-Temporal Encoder and computing the edge embeddings, we utilize the predicted normal edge statistics from NSEM to perform whitening on the edge embeddings using Equation (13). The whitened edge embeddings are then fed into the Anomaly Detector to compute anomaly scores:

$$f(e_{ij}^t) = \sigma(\phi_a(\tilde{\mathbf{z}}_{ij}^t) + \mathbf{b}), \quad (24)$$

where $\phi_a(\cdot)$ is an MLP, \mathbf{b} is a learnable bias term, and $\sigma(\cdot)$ denotes the sigmoid activation function.

Following previous works [13, 22], we employ negative sampling to generate pseudo-anomalous edges for training. Specifically, pseudo anomalies are created by either randomly connecting non-existent edges [22] or randomly altering the destination nodes of existing edges [43]. With the generated pseudo labels, the Anomaly Detector is trained using a binary cross-entropy (BCE) loss defined as

$$\mathcal{L}_{\text{bce}} = - \sum_{e_{ij}^t \in \mathcal{E}^t} \{(1 - y_{ij}^t) \log(1 - f(e_{ij}^t)) + y_{ij}^t \log(f(e_{ij}^t))\}, \quad (25)$$

where y_{ij}^t is the given pseudo label of the edge e_{ij}^t .

4.4 Training Procedure

To avoid the instability caused by continuously changing embeddings and their corresponding statistics during training, we do not train WhENDS in an end-to-end manner. Instead, we adopt a sequential training strategy, where each module is trained independently.

We begin by training the Spatial-Temporal Encoder on the original training set by minimizing the reconstruction loss $\mathcal{L}_{\text{recon}}$, until it can effectively capture the spatial-temporal structure of dynamic graphs. Once the encoder is trained, we apply the data augmentation strategy described earlier: For each snapshot in the training set, we randomly insert 1% to 10% of synthetic edges to simulate the anomalous edge distribution $\mathcal{D}_{\text{ano}}^t$ encountered during testing. During the training of NSEM, for each timestamp t , we compute

the statistics of overall edge embeddings ($\mu_{\text{all}}^t, \Sigma_{\text{all}}^t$) and the ground-truth statistics of normal edge embeddings ($\mu_{\text{norm}}^t, \Sigma_{\text{norm}}^t$) by

$$\mu_{\text{all}}^t = \frac{1}{|\mathcal{E}^t|} \sum_{e_{ij}^t \in \mathcal{E}^t} \mathbf{z}_{ij}^t, \quad (26)$$

$$\Sigma_{\text{all}}^t = \frac{1}{|\mathcal{E}^t|} \sum_{e_{ij}^t \in \mathcal{E}^t} (\mathbf{z}_{ij}^t - \mu_{\text{all}}^t)(\mathbf{z}_{ij}^t - \mu_{\text{all}}^t)^\top, \quad (27)$$

$$\mu_{\text{norm}}^t = \frac{1}{|\mathcal{E}_{\text{norm}}^t|} \sum_{e_{ij}^t \in \mathcal{E}_{\text{norm}}^t} \mathbf{z}_{ij}^t, \quad (28)$$

$$\Sigma_{\text{norm}}^t = \frac{1}{|\mathcal{E}_{\text{norm}}^t|} \sum_{e_{ij}^t \in \mathcal{E}_{\text{norm}}^t} (\mathbf{z}_{ij}^t - \mu_{\text{norm}}^t)(\mathbf{z}_{ij}^t - \mu_{\text{norm}}^t)^\top. \quad (29)$$

The ($\mu_{\text{all}}^t, \Sigma_{\text{all}}^t$) are then used as inputs to NSEM to predict ($\hat{\mu}_{\text{norm}}^t, \hat{\Sigma}_{\text{norm}}^t$), and ($\mu_{\text{norm}}^t, \Sigma_{\text{norm}}^t$) are used to calculate $\mathcal{L}_{\text{statistics}}$ by Equation (14) to train NSEM.

Finally, for Anomaly Detector training, we generate pseudo-anomalous edges via negative sampling on the original training set. Unlike in the testing phase, where the whitening transformation is performed using the predicted statistics from NSEM, during training, we directly use the ground-truth statistics calculated by Equations (28)–(29) to whiten edge embeddings:

$$\tilde{\mathbf{z}}_{ij}^t = (\Sigma_{\text{norm}}^t)^{-\frac{1}{2}} (\mathbf{z}_{ij}^t - \mu_{\text{norm}}^t). \quad (30)$$

The whitened edge embeddings are then fed into the Anomaly Detector to compute anomaly scores by Equation (24), and the model is trained using the binary cross-entropy loss \mathcal{L}_{bce} with pseudo labels, which are calculated by Equation (25).

Since $\mathcal{L}_{\text{recon}}$, $\mathcal{L}_{\text{statistics}}$, and \mathcal{L}_{bce} are used to independently train different components, no loss weight tuning is required. We also summarize the overall training procedure in Algorithm 1.

4.5 Complexity Analysis

In this subsection, we briefly analyze the time complexity of each module of WhENDS.

For the Spatial-Temporal Encoder, the time complexity for an L -layer GraphSAGE [14], which samples uniformly a fixed number k of 1-hop neighbors, is $O(Ld^2k^L)$ [13]. In a single-step LSTM update, we perform computations using GraphSAGE and matrix multiplications. The time complexity for one update is therefore $O(Ld^2k^L + d^2) = O(Ld^2k^L)$.

For reconstruction, given a graph with n nodes, the complexity is $O(nd^2 + n^2d)$ per snapshot, resulting in a total reconstruction cost of $O((nd^2 + n^2d)T)$ over T timestamps.

For the NSEM, we flatten the covariance matrix and concatenate it with the mean vector, forming an input of dimension approximately d^2 . The computational complexity of both the MLP and GRU operations is $O(d^4)$. For a snapshot with e edges, performing whitening on all edge embeddings requires $O(ed^2)$. Thus, the total time complexity of NSEM is $O((d^2 + e)d^2T)$.

For the Anomaly Detector, given T snapshots each with e edges, the total complexity is $O(ed^2T)$.

Putting all components together, the overall time complexity of WhENDS is $O((Lk^L + e + n + d^2)d^2T)$. Since Lk^L is typically small

Algorithm 1 Training Procedure of WhENDS

Input: Dynamic Graph $\mathbb{G} = \{\mathcal{G}^1, \dots, \mathcal{G}^T\}$, training epochs I_e, I_n, I_a

- 1: Initialize network parameters;
- 2: **for** $i = 1$ to I_e **do**
- 3: **for** $t = 1$ to T **do**
- 4: Encode graph representation using Equations (16)–(21)
- 5: Calculate $\mathcal{L}_{\text{recon}}$ using Equations (22)–(23)
- 6: Backpropagate and update parameters of the Spatial-Temporal Encoder
- 7: **end for**
- 8: **end for**
- 9: Inject edges into \mathbb{G}
- 10: **for** $i = 1$ to I_n **do**
- 11: **for** $t = 1$ to T **do**
- 12: Encode graph representation using Equations (16)–(21)
- 13: Calculate statistics of overall edge embeddings using Equations (26)–(27)
- 14: Calculate statistics of normal edge embeddings using Equations (28)–(29)
- 15: Predict normal statistics using Equations (5)–(7)
- 16: Update hidden state using Equations (8)–(12)
- 17: Calculate $\mathcal{L}_{\text{statistics}}$ using Equation (14)
- 18: Backpropagate and update parameters of NSEM
- 19: **end for**
- 20: **end for**
- 21: Generate pseudo anomalies in \mathbb{G}
- 22: **for** $i = 1$ to I_a **do**
- 23: **for** $t = 1$ to T **do**
- 24: Encode graph representation using Equations (16)–(21)
- 25: Calculate statistics of normal edge embeddings using Equations (28)–(29)
- 26: Whiten edge embeddings using Equation (30)
- 27: Calculate anomaly score $f(e_{ij}^t)$ using Equation (24)
- 28: Calculate \mathcal{L}_{bce} using Equation (25)
- 29: Backpropagate and update parameters of Anomaly Detector
- 30: **end for**
- 31: **end for**

Table 1: Dataset statistics.

Dataset	Nodes	Edges	Avg.Degree
UCI Messages	1,899	13,838	14.57
Digg	30,360	85,155	5.61
Bitcoin-Alpha	3,777	24,173	12.80
Bitcoin-OTC	5,881	35,588	12.10

in practice, it can be considered negligible. Therefore, the simplified overall complexity of WhENDS becomes $O(ed^2T + nd^2T + d^4T)$.

5 Experiments

5.1 Experiment Setup

Datasets. We evaluate the performance of our model on four widely used dynamic graph anomaly detection datasets. Summary statistics are provided in Table 1.

UCI Messages [24] records a directed communication network among users of an online student community at the University of California, Irvine. Each node represents a user, and each directed edge corresponds to a message sent from one user to another.

Digg [9] captures user interactions on the social news platform Digg. Nodes correspond to users, and a directed edge indicates that one user replied to another user’s comment or post.

Bitcoin-Alpha [19] represents a who-trusts-whom network collected from the Bitcoin-Alpha trading platform. Each node denotes a trader, and an edge indicates that a user assigned a trust rating to another user.

Bitcoin-OTC [18] is another who-trusts-whom network, collected from the Bitcoin OTC trading platform. Similar to Bitcoin-Alpha, nodes represent users and edges indicate directed trust ratings between users.

Baselines. We compare our method against nine state-of-the-art baseline approaches, which can be grouped into the following three categories:

(1) *Classical Anomaly Scoring Methods:* **Sedanspot** [10] detects anomalies using a random walk-based holistic scoring function that captures changes in connectivity patterns. **CM-Sketch** [27] applies the Count-Min Sketch algorithm to approximate empirical anomaly metrics and identify anomalous edges.

(2) *Graph Embedding Methods:* **Spectral Clustering** [30] learns node embeddings by maximizing local neighborhood similarity via spectral decomposition of the adjacency matrix. **DeepWalk** [25] generates node embeddings using the Skip-gram model applied to random walks sampled from the graph structure.

(3) *Deep Anomaly Detection Methods:* **NetWalk** [34] adopts a reconstruction-based strategy, training an autoencoder on random walk sequences to generate node and edge embeddings, and computing anomaly scores via clustering. **AddGraph** [43] constructs h -hop enclosing subgraphs for each edge and applies a spatial-temporal model to learn discriminative edge embeddings. **TADDY** [22] employs edge-based substructure sampling combined with advanced node embeddings as input to a transformer-based model for dynamic anomaly detection. **RustGraph** [13] integrates GNNs with GRUs to capture spatial-temporal dependencies and leverages graph contrastive learning to encode dynamic graphs.

Experiment Details. We follow previous works [13] for data pre-processing and use `node2vec` [12] to generate raw features for each node. For each dataset, the first 50% of the snapshots are used as the training set, while the remaining 50% are used as the testing set. To evaluate model performance under different anomaly rates, we inject anomalous edges into the test set with three different proportions (1%, 5%, 10%).

Metric. We adopt the Area Under the Receiver Operating Characteristic Curve (AUC-ROC) as the primary metric to evaluate model performance. The AUC-ROC score ranges from 0 to 1, where a higher score indicates better anomaly detection performance.

Table 2: Anomaly detection results reported using the AUC-ROC score. The best result in each column is highlighted in bold, and the second-best is underlined.

Methods	UCI Messages			Digg			Bitcoin-Alpha			Bitcoin-OTC		
	1%	5%	10%	1%	5%	10%	1%	5%	10%	1%	5%	10%
Sedanspot	0.7342	0.7156	0.7061	0.6976	0.6784	0.6396	0.7380	0.7264	0.7085	0.7346	0.7284	0.7156
CM-Sketch	0.7320	0.6968	0.6835	0.6884	0.6675	0.6358	0.7146	0.7015	0.6887	0.7412	0.7338	0.7242
Spectral Clustering	0.6324	0.6104	0.5794	0.5949	0.5823	0.5591	0.7401	0.7275	0.7167	0.7624	0.7376	0.7047
DeepWalk	0.7514	0.7391	0.6979	0.7080	0.6881	0.6396	0.6985	0.6874	0.6793	0.7423	0.7356	0.7287
NetWalk	0.7758	0.7647	0.7226	0.7563	0.7176	0.6837	0.8385	0.8357	0.8350	0.7785	0.7694	0.7534
AddGraph	0.8083	0.8090	0.7688	0.8341	0.8470	0.8369	0.8665	0.8403	0.8498	0.8352	0.8455	0.8592
StrGNN	0.8179	0.8252	0.7959	0.8162	0.8254	0.8272	0.8574	0.8667	0.8627	0.9012	0.8775	0.8836
TADDY	0.8912	0.8398	0.8370	0.8617	0.8545	0.8440	<u>0.9451</u>	0.9341	0.9423	0.9455	0.9340	0.9425
RustGraph	<u>0.9128</u>	<u>0.9117</u>	<u>0.9124</u>	<u>0.8795</u>	<u>0.8577</u>	<u>0.8624</u>	0.9447	<u>0.9348</u>	0.9207	<u>0.9608</u>	<u>0.9578</u>	<u>0.9603</u>
WhENDS	0.9660	0.9627	0.9584	0.8810	0.8708	0.8678	0.9736	0.9610	<u>0.9416</u>	0.9721	0.9728	0.9713

Parameter Setting. For all datasets, we set the embedding dimension to $d = 128$. To ensure fair comparisons, following previous work [34], we set the snapshot size to 1,000 for UCI Messages and Bitcoin-OTC, 2,000 for Bitcoin-Alpha, and 6,000 for Digg.

All GNN and MLP components are implemented with two layers, and we use GraphSAGE [14] as the GNN encoder in our work. The NSEM utilizes a two-layer GRU, and the Spatial-Temporal Encoder is constructed with two layers of the LSTM-based structure described earlier.

During training, the hyperparameters are configured as follows:

- **Spatial-Temporal Encoder:** UCI Messages and Digg: 200 epochs, learning rate 0.0005; Bitcoin-Alpha: 100 epochs, learning rate 0.0005; Bitcoin-OTC: 100 epochs, learning rate 0.0001.
- **NSEM:** All datasets: 200 epochs, learning rate 0.001.
- **Anomaly Detector:** UCI Messages: 800 epochs, learning rate 0.001; Digg: 1600 epochs, learning rate 0.001; Bitcoin-Alpha: 800 epochs, learning rate 0.001; Bitcoin-OTC: 1600 epochs, learning rate 0.0005.

All modules are optimized using the Adam optimizer, with the weight decay rate set to 0.9.

5.2 Anomaly Detection Results

Anomaly detection results on the four datasets are reported in Table 2, from which we draw the following observations:

- WhENDS achieves state-of-the-art results in most of the 12 experimental settings. Compared with the best-performing baselines, it yields an average improvement of 2.36%, demonstrating the effectiveness of our method and underscoring the importance of addressing NDS in anomaly detection.
- The performance gain of WhENDS varies across datasets. The average improvements on UCI Messages, Digg, Bitcoin-Alpha, and Bitcoin-OTC are 5.38%, 0.77%, 1.91%, and 1.29%, respectively. This variation is likely due to different degrees of NDS present in each dataset.

- WhENDS shows larger improvements in settings with sparser anomalies. At anomaly ratios of 1%, 5%, and 10%, the average AUC-ROC gains are 2.56%, 2.88%, and 1.65%, respectively. We attribute this to WhENDS’s whitening-based alignment, which effectively standardizes normal edge distributions across time, enhancing its ability to detect subtle anomalies even when they are scarce.

5.3 Ablation Study

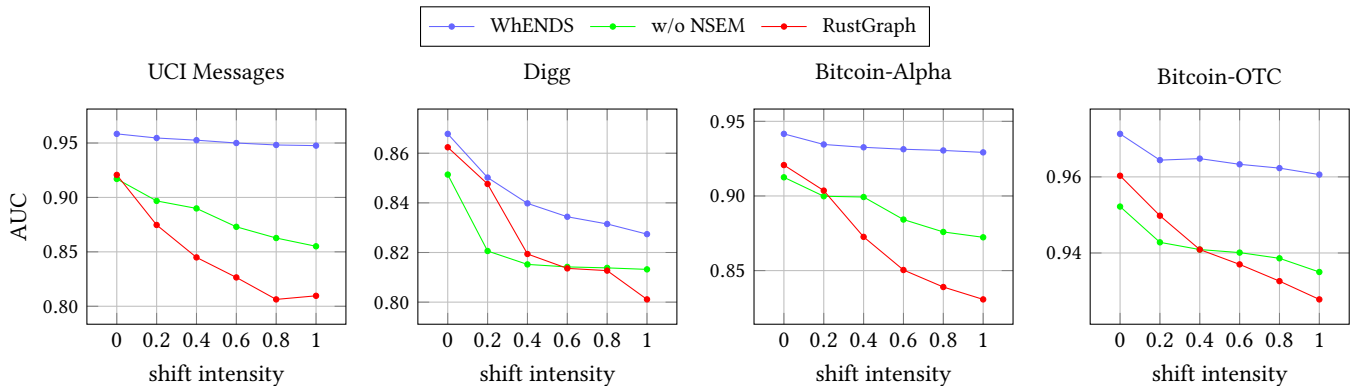
We conduct an ablation study to investigate the contribution of each component in our model. Specifically, in **w/o ST Encoder**, we replace the Spatial-Temporal Encoder with a simple two-layer GNN, so the model can only capture structural information and loses the ability to model temporal dynamics. In **w/o GRU**, we remove the GRU component from NSEM, preventing it from learning the temporal evolution patterns of normal distributions. In **w/o DataAug**, we disable data augmentation during the training of NSEM. In this setting, NSEM directly predicts the normal statistics from the previous hidden state h_s^{t-1} , rather than predicting the deviation between the overall and normal edge embedding statistics. In **w/o NSEM**, we remove the entire NSEM module, and thus no whitening is applied to the edge embeddings, leaving the model unable to handle NDS.

The results of the ablation study are shown in Table 3, from which we draw the following conclusions:

- NSEM is the most critical component of WhENDS. In all datasets, removing NSEM results in the worst performance among all ablated variants, leading to an average drop in AUC-ROC score of 3.69%, which demonstrates the effectiveness of NSEM.
- Among the components of NSEM, data augmentation proves to be the most influential. Disabling data augmentation results in an average drop in AUC-ROC of 2.69%, whereas removing the GRU while retaining data augmentation leads to negligible performance differences in UCI Messages, Digg,

Table 3: The ablation study results are reported using the AUC-ROC score. The best result in each column is highlighted in bold, and the second-best is underlined.

Methods	UCI Messages			Digg			Bitcoin-Alpha			Bitcoin-OTC		
	1%	5%	10%	1%	5%	10%	1%	5%	10%	1%	5%	10%
WhENDS	<u>0.9660</u>	0.9627	0.9584	<u>0.8810</u>	0.8708	<u>0.8678</u>	0.9736	0.9610	0.9416	<u>0.9721</u>	0.9728	0.9713
w/o ST Encoder	0.9315	0.9317	0.9264	0.8533	0.8514	0.8562	0.9486	0.9360	0.9160	0.9430	0.9483	0.9369
w/o GRU	0.9669	<u>0.9626</u>	<u>0.9582</u>	0.8811	<u>0.8705</u>	0.8684	<u>0.9633</u>	<u>0.9468</u>	<u>0.9388</u>	0.9730	<u>0.9727</u>	<u>0.9711</u>
w/o DataAug	0.9315	0.9317	0.9264	0.8651	0.8557	0.8566	0.9450	0.9262	0.9133	0.9538	0.9456	0.9567
w/o NSEM	0.9170	0.9137	0.9132	0.8514	0.8319	0.8386	0.9407	0.9287	0.9125	0.9345	0.9375	0.9367

**Figure 4: The AUC-ROC curves under different intensity of normality distribution shift.**

and Bitcoin-OTC. This suggests that, in most cases, NSEM is able to rely solely on data augmentation to make accurate predictions.

- In Bitcoin-Alpha, removing the GRU results in a decrease in AUC-ROC of up to 1.42%. We attribute this to the mismatch between the synthetic anomalies introduced by data augmentation and the actual anomalous edges in the test set, as previously discussed. This result also suggests that learning evolution patterns of distribution helps mitigate the adverse effects caused by this mismatch. Moreover, although using the GRU alone without data augmentation leads to a performance drop of 2.43%, it still achieves competitive results, demonstrating that learning distributional evolution alone can provide reasonably effective predictions.
- Replacing the Spatial-Temporal Encoder with a simple GNN causes an average decrease in AUC-ROC of 2.68%, indicating the importance of capturing temporal information for anomaly detection in dynamic graphs, as also supported by previous studies [13, 22].

5.4 Impact of Normality Distribution Shift

To verify the impact of normality distribution shift on anomaly detection model performance, we design a controlled experiment by artificially introducing varying degrees of normality distribution shift into the datasets.

Specifically, since the original datasets do not contain raw node features, we first use node2vec to generate initial node features, denoted as X^0 , and assign them as the node features for the graph snapshot \mathcal{G}^0 at timestamp $t = 0$.

For each subsequent timestamp $t > 0$, the node features X^t are generated by adding Gaussian noise with standard deviation σ to the node features from the previous timestamp X^{t-1} :

$$X^t = X^{t-1} + \sigma \epsilon^t, \quad \epsilon^t \sim \mathcal{N}(0, I), \quad (31)$$

where I is the identity matrix, and ϵ^t is sampled independently for each node at each timestamp.

By introducing perturbations to the node features over time, we indirectly induce a shift in the edge distribution, thereby simulating the effect of NDS in dynamic graphs. After introducing the perturbations, we insert 10% anomalous edges into each test set to evaluate anomaly detection performance under the shifted distributions. By adjusting σ , we control the strength of the injected distribution shift. We conduct experiments with $\sigma \in \{0.2, 0.4, 0.6, 0.8, 1.0\}$ to evaluate model robustness under different shift intensities.

We compare our proposed method with two baselines: RustGraph and our method without the NSEM module (w/o NSEM). For RustGraph [13], we use their public code to re-run the experiment. The experimental results are shown in Figure 4, from which we summarize the following findings:

- Compared to RustGraph and the variant without NSEM, WhENDS consistently achieves the best performance across

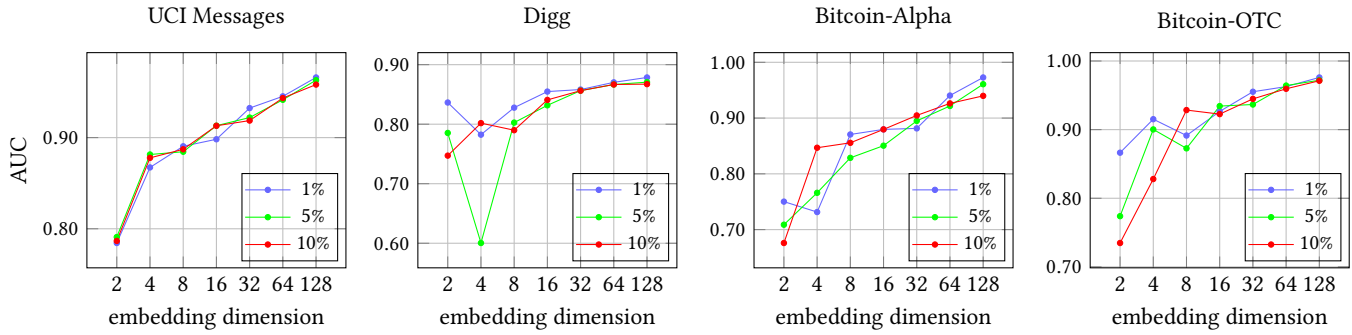


Figure 5: Sensitivity analysis results for the embedding dimension. Results are reported using the AUC-ROC score.

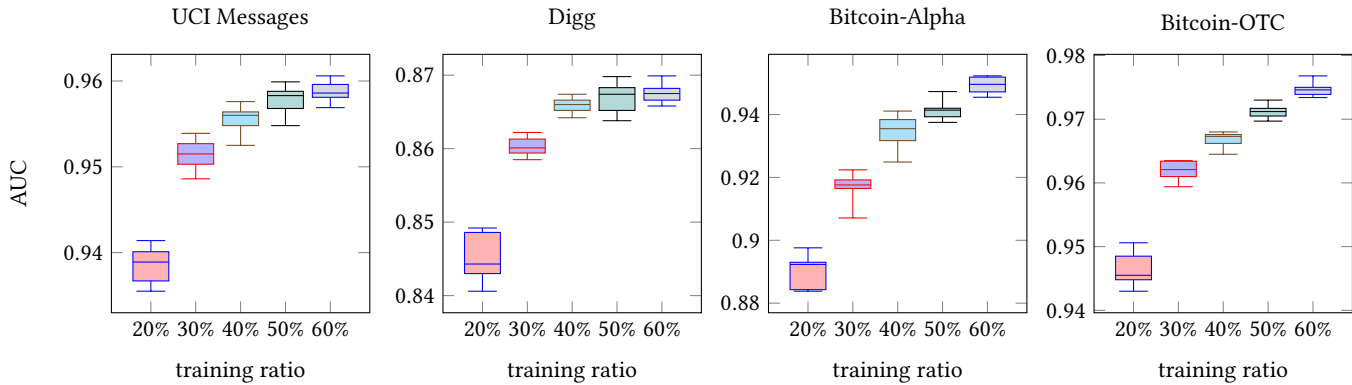


Figure 6: Sensitivity analysis results with different training ratios.

all experiments. As the intensity of NDS increases, WhENDS maintains relatively stable performance, and even under strong NDS, it continues to outperform other models, demonstrating its robustness to NDS.

- The NSEM module plays a critical role in mitigating the effects of NDS. Removing NSEM leads to significant performance degradation and a noticeable loss of stability under increasing NDS intensity, especially in UCI Messages and Bitcoin-Alpha.
- The model without NSEM still exhibits a certain level of robustness as the intensity of NDS increases. We attribute this to the numerically stable design of the Spatial-Temporal Encoder, which helps prevent excessive fluctuations in embedding values under large distribution shifts, thereby preserving some level of performance stability.

5.5 Sensitivity Analysis

We further conduct sensitivity analysis to investigate the impact of different hyperparameters on our model’s performance. Specifically, we evaluate the effects of varying the embedding dimension d and the training ratio. Experiments are conducted on all four datasets, and for each test set, we inject 10% anomalous edges to evaluate model performance.

Embedding Dimension d . To investigate the effect of the embedding dimension, we vary d across $\{2, 4, 8, 16, 32, 64, 128\}$ and evaluate model performance on all datasets. As shown in Figure 5, the model performance generally improves as the embedding dimension increases. This indicates that a higher-dimensional embedding space allows the model to capture more informative representations, leading to better anomaly detection performance.

Training Ratio. To evaluate the effect of different training ratios, we conduct experiments with training ratios of $\{20\%, 30\%, 40\%, 50\%, 60\%\}$, and the results are summarized in Figure 6. The experimental results show that WhENDS benefits from higher training ratios, with its performance improving as more training data becomes available. When the training ratio is low, WhENDS performs well on datasets with a larger number of snapshots, such as UCI Messages and Bitcoin-OTC, but struggles on Digg and Bitcoin-Alpha, where the number of snapshots is relatively limited. We attribute this to the training strategy of the NSEM module. When there are sufficient snapshots, NSEM has access to a larger number of statistical samples across timestamps, which enables more effective learning of the statistics of normal edge embeddings. In contrast, with fewer snapshots, the statistics available at each timestamp are limited, making it difficult to accurately estimate the statistics of normal edge embeddings, and leading to suboptimal performance of WhENDS.

6 Conclusion

In this paper, we identified normality distribution shift (NDS) as a fundamental challenge for anomaly detection in dynamic graphs, demonstrating that NDS can cause models to misclassify normal instances, thereby degrading performance and reducing robustness over time. To address this issue, we proposed **WhENDS**, a novel unsupervised anomaly detection method that mitigates the effects of NDS by aligning normal edge embeddings across timestamps to a standard Gaussian distribution via a whitening transformation. Extensive experiments demonstrate that WhENDS consistently outperforms strong baselines and remains robust under varying degrees of distribution shift.

Our model does not rely on any personally identifiable information or private attributes, and our experiments are conducted on publicly available benchmark datasets.

References

- [1] Charu C. Aggarwal, Yuchen Zhao, and Philip S. Yu. Outlier detection in graph streams. In *2011 IEEE 27th International Conference on Data Engineering*, pages 399–409, 2011.
- [2] Jerome H. Friedman and. Exploratory projection pursuit. *Journal of the American Statistical Association*, 82(397):249–266, 1987.
- [3] Maximilian Beck, Korbinian Pöppel, Markus Spanring, Andreas Auer, Oleksandra Prudnikova, Michael Kopp, Günter Klambauer, Johannes Brandstetter, and Sepp Hochreiter. xlstm: Extended long short-term memory, 2024.
- [4] Tanya Y. Berger-Wolf and Jared Saia. A framework for analysis of dynamic social networks. In *Proceedings of the 12th ACM SIGKDD International Conference on Knowledge Discovery and Data Mining*, KDD '06, page 523–528, New York, NY, USA, 2006. Association for Computing Machinery.
- [5] Lei Cai, Zhengzhang Chen, Chen Luo, Jiaping Gui, Jingchao Ni, Ding Li, and Haifeng Chen. Structural temporal graph neural networks for anomaly detection in dynamic graphs. In *Proceedings of the 30th ACM International Conference on Information & Knowledge Management*, CIKM '21, page 3747–3756, New York, NY, USA, 2021. Association for Computing Machinery.
- [6] Varun Chandola, Arindam Banerjee, and Vipin Kumar. Anomaly detection: A survey. *ACM Comput. Surv.*, 41(3), July 2009.
- [7] Jinyin Chen, Xueke Wang, and Xuanheng Xu. Gc-lstm: graph convolution embedded lstm for dynamic network link prediction. *Applied Intelligence*, 52(7):7513–7528, May 2022.
- [8] Kyunghyun Cho, Bart van Merriënboer, Caglar Gulcehre, Dzmitry Bahdanau, Fethi Bougares, Holger Schwenk, and Yoshua Bengio. Learning phrase representations using rnn encoder-decoder for statistical machine translation, 2014.
- [9] Munmun De Choudhury, Hari Sundaram, Ajita John, and Dorée Duncan Seligmann. Social synchrony: Predicting mimicry of user actions in online social media. In *2009 International Conference on Computational Science and Engineering*, volume 4, pages 151–158, 2009.
- [10] Dhivya Eswaran and Christos Faloutsos. Sedanspot: Detecting anomalies in edge streams. In *2018 IEEE International Conference on Data Mining (ICDM)*, pages 953–958, 2018.
- [11] Wenzheng Feng, Jie Zhang, Yuxiao Dong, Yu Han, Huanbo Luan, Qian Xu, Qiang Yang, Evgeny Kharlamov, and Jie Tang. Graph random neural network for semi-supervised learning on graphs, 2021.
- [12] Aditya Grover and Jure Leskovec. node2vec: Scalable feature learning for networks. In *Proceedings of the 22nd ACM SIGKDD International Conference on Knowledge Discovery and Data Mining*, KDD '16, page 855–864, New York, NY, USA, 2016. Association for Computing Machinery.
- [13] Jianhao Guo, Siliang Tang, Juncheng Li, Kaihang Pan, and Lingfei Wu. Rustgraph: Robust anomaly detection in dynamic graphs by jointly learning structural-temporal dependency. *IEEE Transactions on Knowledge and Data Engineering*, 36(7):3472–3485, 2024.
- [14] William L. Hamilton, Rex Ying, and Jure Leskovec. Inductive representation learning on large graphs, 2018.
- [15] Weihua Hu, Bowen Liu, Joseph Gomes, Marinka Zitnik, Percy Liang, Vijay Pande, and Jure Leskovec. Strategies for pre-training graph neural networks, 2020.
- [16] Thomas N. Kipf and Max Welling. Variational graph auto-encoders, 2016.
- [17] Thomas N. Kipf and Max Welling. Semi-supervised classification with graph convolutional networks, 2017.
- [18] Srijan Kumar, Bryan Hooi, Disha Makhija, Mohit Kumar, Christos Faloutsos, and V.S. Subrahmanian. Rev2: Fraudulent user prediction in rating platforms. In *Proceedings of the Eleventh ACM International Conference on Web Search and Data Mining*, WSDM '18, page 333–341, New York, NY, USA, 2018. Association for Computing Machinery.
- [19] Srijan Kumar, Francesca Spezzano, V. S. Subrahmanian, and Christos Faloutsos. Edge weight prediction in weighted signed networks. In *2016 IEEE 16th International Conference on Data Mining (ICDM)*, pages 221–230, 2016.
- [20] Fuxian Li, Jie Feng, Huan Yan, Guangyin Jin, Fan Yang, Funing Sun, Depeng Jin, and Yong Li. Dynamic graph convolutional recurrent network for traffic prediction: Benchmark and solution. *ACM Trans. Knowl. Discov. Data*, 17(1), February 2023.
- [21] Haoyang Li, Xin Wang, Ziwei Zhang, and Wenwu Zhu. Ood-gnn: Out-of-distribution generalized graph neural network. *IEEE Transactions on Knowledge and Data Engineering*, 35(7):7328–7340, 2023.
- [22] Yixin Liu, Shirui Pan, Yu Guang Wang, Fei Xiong, Liang Wang, Qingfeng Chen, and Vincent CS Lee. Anomaly detection in dynamic graphs via transformer. *IEEE Transactions on Knowledge and Data Engineering*, 35(12):12081–12094, December 2023.
- [23] Jianxin Ma, Peng Cui, Kun Kuang, Xin Wang, and Wenwu Zhu. Disentangled graph convolutional networks. In Kamalika Chaudhuri and Ruslan Salakhutdinov, editors, *Proceedings of the 36th International Conference on Machine Learning*, volume 97 of *Proceedings of Machine Learning Research*, pages 4212–4221. PMLR, 09–15 Jun 2019.
- [24] Tore Opsahl and Pietro Panzarasa. Clustering in weighted networks. *Social Networks*, 31(2):155–163, 2009.
- [25] Bryan Perozzi, Rami Al-Rfou, and Steven Skiena. Deepwalk: online learning of social representations. In *Proceedings of the 20th ACM SIGKDD International Conference on Knowledge Discovery and Data Mining*, KDD '14, page 701–710, New York, NY, USA, 2014. Association for Computing Machinery.
- [26] Tiexin Qin, Shiqi Wang, and Haoliang Li. Generalizing to evolving domains with latent structure-aware sequential autoencoder, 2022.
- [27] Stephen Ranshous, Steve Harenberg, Kshitij Sharma, and Nagiza F. Samatova. *A Scalable Approach for Outlier Detection in Edge Streams Using Sketch-based Approximations*, pages 189–197.
- [28] Xiao Shen, Dewang Sun, Shirui Pan, Xi Zhou, and Laurence T. Yang. Neighbor contrastive learning on learnable graph augmentation, 2023.
- [29] Ashish Vaswani, Noam Shazeer, Niki Parmar, Jakob Uszkoreit, Llion Jones, Aidan N. Gomez, Lukasz Kaiser, and Illia Polosukhin. Attention is all you need, 2023.
- [30] Ulrike von Luxburg. A tutorial on spectral clustering, 2007.
- [31] Liang Wang, Zhiwen Yu, Fei Xiong, Dingqi Yang, Shirui Pan, and Zheng Yan. Influence spread in geo-social networks: A multiobjective optimization perspective. *IEEE Transactions on Cybernetics*, 51(5):2663–2675, 2021.
- [32] Mixue Xie, Shuang Li, Longhui Yuan, Chi Liu, and Zehui Dai. Evolving standardization for continual domain generalization over temporal drift. In A. Oh, T. Naumann, A. Globerson, K. Saenko, M. Hardt, and S. Levine, editors, *Advances in Neural Information Processing Systems*, volume 36, pages 21983–22002. Curran Associates, Inc., 2023.
- [33] Yuning You, Tianlong Chen, Yongduo Sui, Ting Chen, Zhangyang Wang, and Yang Shen. Graph contrastive learning with augmentations, 2021.
- [34] Wenchao Yu, Wei Cheng, Charu C. Aggarwal, Kai Zhang, Haifeng Chen, and Wei Wang. Netwalk: A flexible deep embedding approach for anomaly detection in dynamic networks. In *Proceedings of the 24th ACM SIGKDD International Conference on Knowledge Discovery & Data Mining*, KDD '18, page 2672–2681, New York, NY, USA, 2018. Association for Computing Machinery.
- [35] Haonan Yuan, Qingyun Sun, Xingcheng Fu, Ziwei Zhang, Cheng Ji, Hao Peng, and Jianxin Li. Environment-aware dynamic graph learning for out-of-distribution generalization. In A. Oh, T. Naumann, A. Globerson, K. Saenko, M. Hardt, and S. Levine, editors, *Advances in Neural Information Processing Systems*, volume 36, pages 49715–49747. Curran Associates, Inc., 2023.
- [36] Qiuhaio Zeng, Wei Wang, Fan Zhou, Charles Ling, and Boyu Wang. Foresee what you will learn: Data augmentation for domain generalization in non-stationary environment, 2023.
- [37] Kexin Zhang, Shuhan Liu, Song Wang, Weili Shi, Chen Chen, Pan Li, Sheng Li, Jundong Li, and Kaize Ding. A survey of deep graph learning under distribution shifts: from graph out-of-distribution generalization to adaptation, 2025.
- [38] Mengqi Zhang, Shu Wu, Xueli Yu, Qiang Liu, and Liang Wang. Dynamic graph neural networks for sequential recommendation, 2021.
- [39] Shengyu Zhang, Yunze Tong, Kun Kuang, Fuli Feng, Jiezhong Qiu, Jin Yu, Zhou Zhao, Hongxia Yang, Zhongfei Zhang, and Fei Wu. Stable prediction on graphs with agnostic distribution shifts. In Thuc Le, Jiuyong Li, Robert Ness, Sofia Triantafillou, Shohei Shimizu, Peng Cui, Kun Kuang, Jian Pei, Fei Wang, and Mattia Proserpi, editors, *Proceedings of The KDD'23 Workshop on Causal Discovery, Prediction and Decision*, volume 218 of *Proceedings of Machine Learning Research*, pages 49–74. PMLR, 07 Aug 2023.
- [40] Zeyang Zhang, Xin Wang, Ziwei Zhang, Haoyang Li, Zhou Qin, and Wenwu Zhu. Dynamic graph neural networks under spatio-temporal distribution shift. In S. Koyejo, S. Mohamed, A. Agarwal, D. Belgrave, K. Cho, and A. Oh, editors, *Advances in Neural Information Processing Systems*, volume 35, pages 6074–6089. Curran Associates, Inc., 2022.

- [41] Zeyang Zhang, Xin Wang, Ziwei Zhang, Zhou Qin, Weigao Wen, Hui Xue', Haoyang Li, and Wenwu Zhu. Spectral invariant learning for dynamic graphs under distribution shifts. In A. Oh, T. Naumann, A. Globerson, K. Saenko, M. Hardt, and S. Levine, editors, *Advances in Neural Information Processing Systems*, volume 36, pages 6619–6633. Curran Associates, Inc., 2023.
- [42] Tong Zhao, Wei Jin, Yozen Liu, Yingheng Wang, Gang Liu, Stephan Günnemann, Neil Shah, and Meng Jiang. Graph data augmentation for graph machine learning: A survey, 2023.
- [43] Li Zheng, Zhenpeng Li, Jian Li, Zhao Li, and Jun Gao. Addgraph: Anomaly detection in dynamic graph using attention-based temporal gcn. In *Proceedings of the Twenty-Eighth International Joint Conference on Artificial Intelligence, IJCAI-19*, pages 4419–4425. International Joint Conferences on Artificial Intelligence Organization, 7 2019.
- [44] Yu Zheng, Ruiqi Hu, Sai-fu Fung, Celina Yu, Guodong Long, Ting Guo, and Shirui Pan. Clustering social audiences in business information networks. *Pattern Recognition*, 100(C), April 2020.